

Supporting Information for

Contribution of anthropogenic aerosols to persistent La Niña-like conditions in the early 21st century

Yen-Ting Hwang¹, Shang-Ping Xie², Po-Ju Chen^{1,3}, Hung-Yi Tseng¹, and Clara Deser⁴

¹Department of Atmospheric Sciences, National Taiwan University, Taipei, Taiwan

²Scripps Institute of Oceanography, University of California San Diego, La Jolla, California, USA

³Department of Atmospheric, Oceanic, & Earth Sciences, George Mason University, Fairfax, Virginia, USA

⁴Climate and Global Dynamics, National Center for Atmospheric Research, Boulder, Colorado, USA

Corresponding authors: Yen-Ting Hwang and Clara Deser

Emails: ythwang@ntu.edu.tw, cdeser@ucar.edu

This PDF file includes:

Supporting text
Figures S1 to S8
SI References

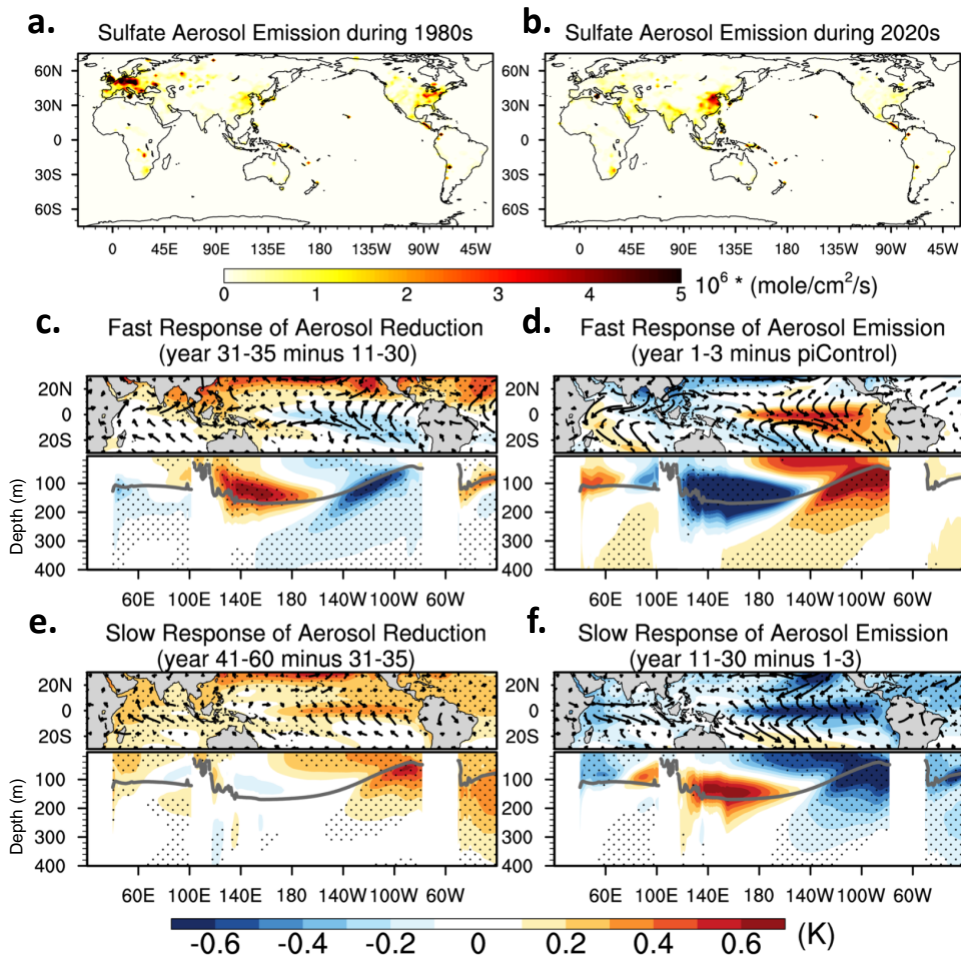


Figure S1. The geographic distribution of sulfate aerosol emission during (a) 1980s and (b) 2020s. (c)(e) The fast and slow responses to sudden removal of the aerosol forcing in the experiment using the sulfate aerosol emission during 1980s. (d)(f) The fast and slow responses in the experiment using the sulfate aerosol emission during 2020s.

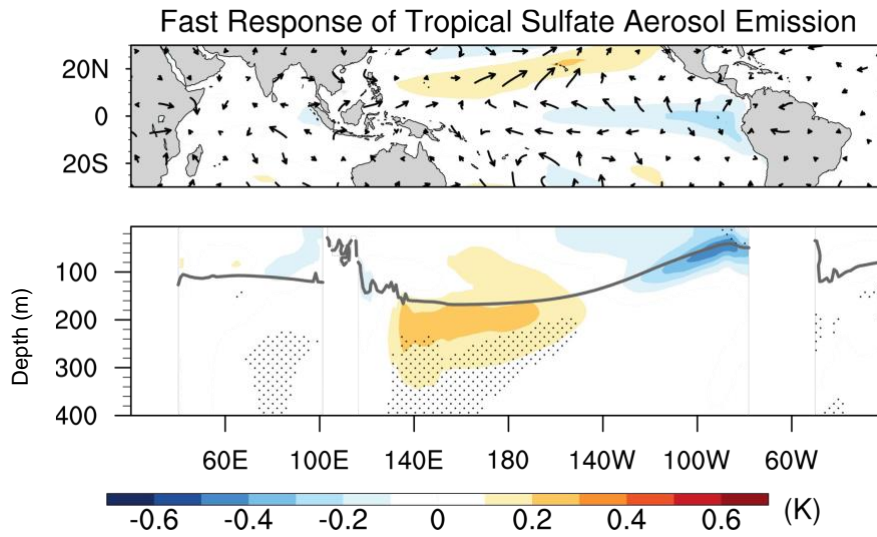


Figure S2. Similar panels to the Figure 3 but for the fast response (year 1-3 minus control) in the idealized aerosol experiments using tropical sulfate aerosol emission. The tropical-only aerosol experiment, containing 15 ensemble members, involved a time invariant sulfate aerosol emission between 10°S~10°N at 1980s condition, which is suddenly introduced in the beginning of the experiment.

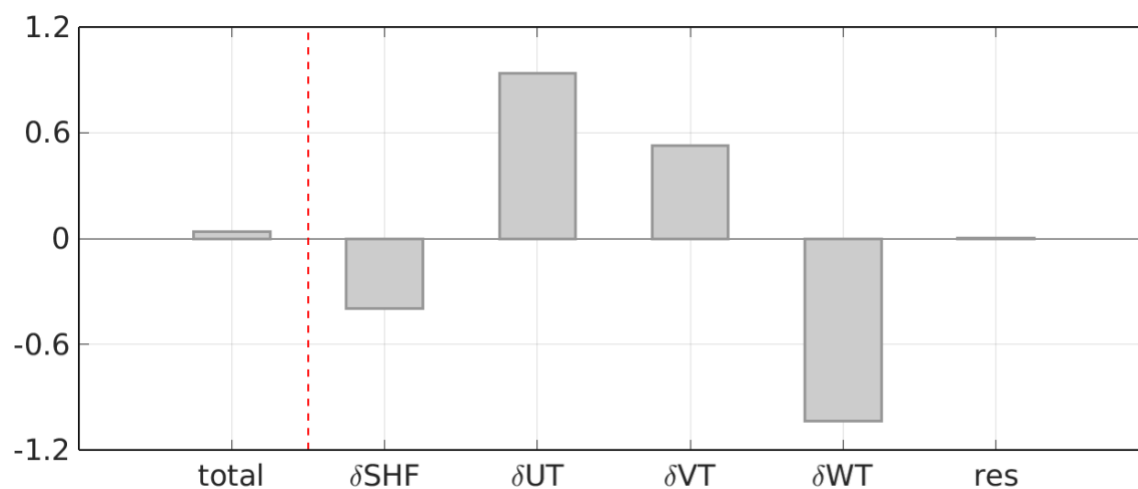


Figure S3. Temporally integrated, anomalous heat budget (in K) in the top 50 meter of equatorial Pacific region (5°S–5°N, 150°E–60°W) during years 1-3. Bars from the left include: the tendency term (total change in oceanic temperature), surface flux, heat convergence from the horizontal, meridional, and vertical directions, and the residual term. Detailed derivation of the heat budget can be found in Eq. 2.2-2.6 in Tseng et al. 2023¹. In brief, the anomalous temperature (relative to control) at year 3 (the first bar on the left) can be attributed to the contributions from the five bars on the right.

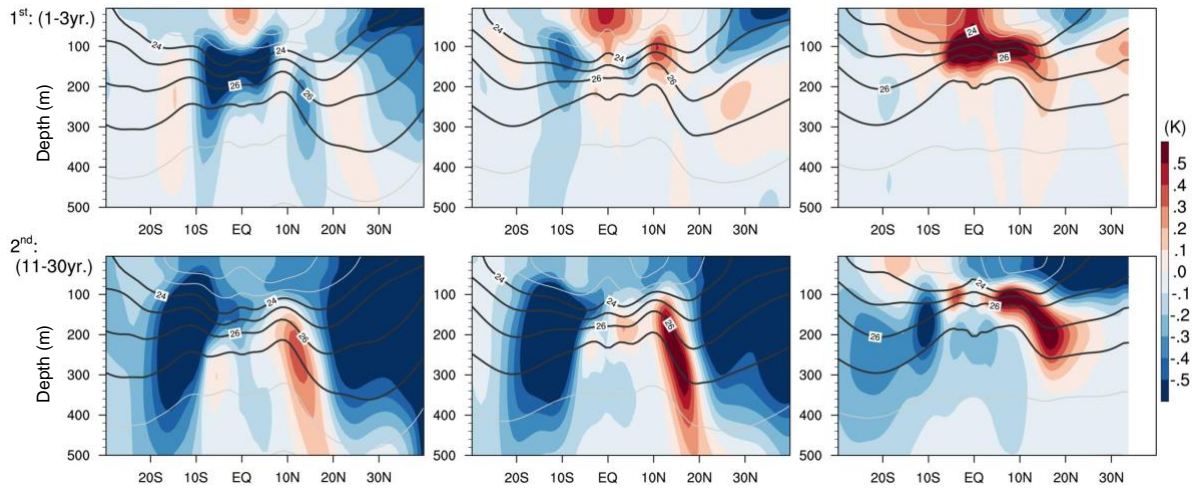


Figure S4. The meridional depth-profile of (top) fast and (bottom) slow potential temperature responses over Pacific in the idealized aerosol experiment. From the left to the right panels, we show the potential temperature anomalies (shaded) at 160°E, 160°W, and 120°W. The light grey lines denote the isopycnals of the control simulation, and the black lines represent the $\sigma_0 = 24\sim 27 \text{ kg/m}^3$ isopycnals.

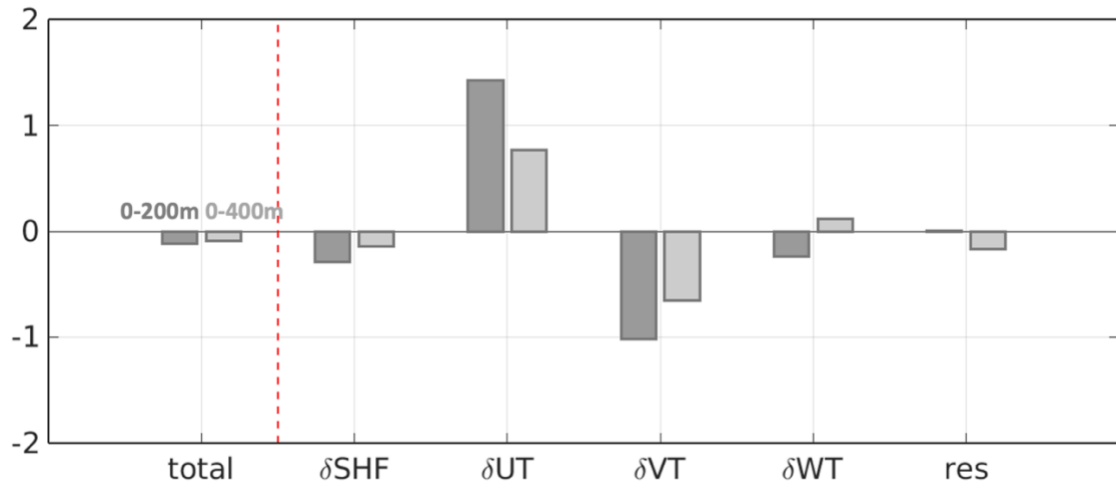


Figure S5. As in Figure S3, but for 0-200m (darker grey bars) and 0-400m (lighter grey bars) heat budgets in degree K in the equatorial Pacific region (5°S–5°N, 150°E-60°W) during years 1–10.

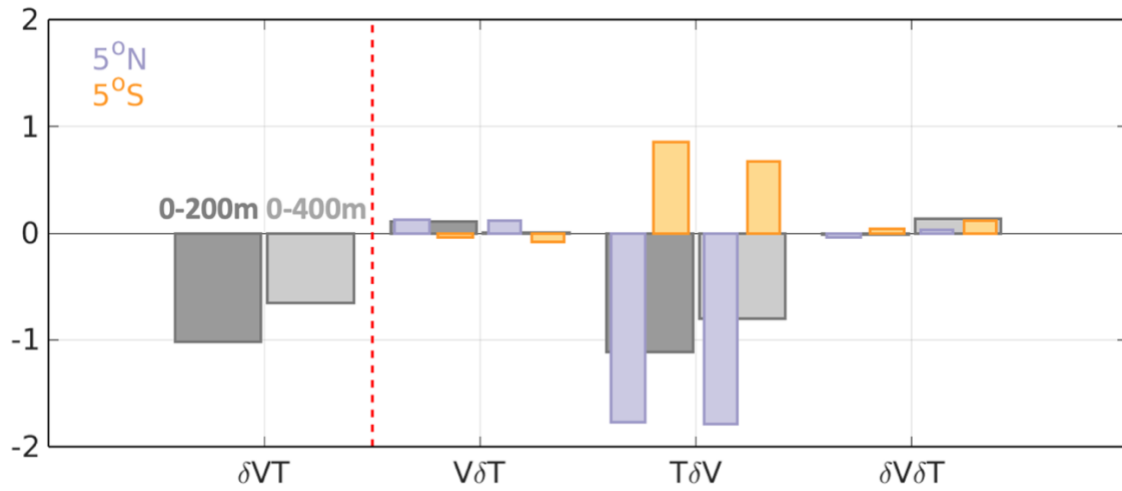


Figure S6. The heat convergence from the meridional convergence (the first two bars on the left, the forth term in Figure S5) is further decomposed into contributions of anomalous temperature, velocity, and a nonlinear term, with the contribution from the northern and the southern boundaries plotted as light purple and light orange bars.

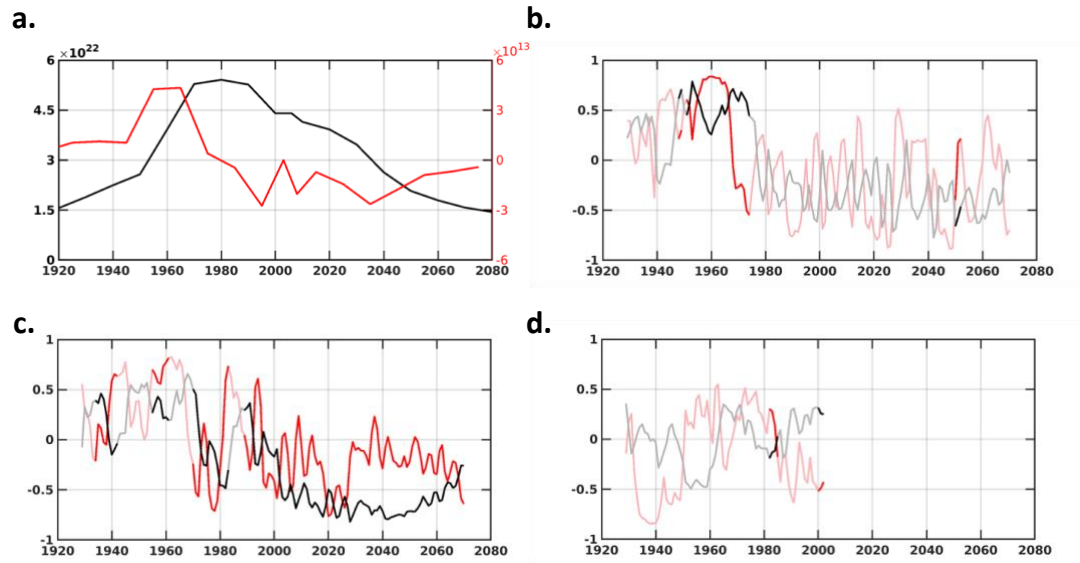


Figure S7. Evolution of (a) the globally averaged sulfate aerosol emission in CESM LE (plotted in black, molecule/cm²/s) and its time differential (plotted in red, molecule/cm²/s²), and the pattern correlation between the 20-year running trend of tropical Pacific SST in (b) ALL minus XAERindus (c) ALL (d) HadISST (observation) and the fast response (plotted in red) and the slow response (plotted in black) in the idealized experiment (the patterns plotted in Figure 3). The light black and red lines in (b)-(d) denote the time that the 20-year SST running trends are not statistically significant over more than 70% of the tropical Pacific region.

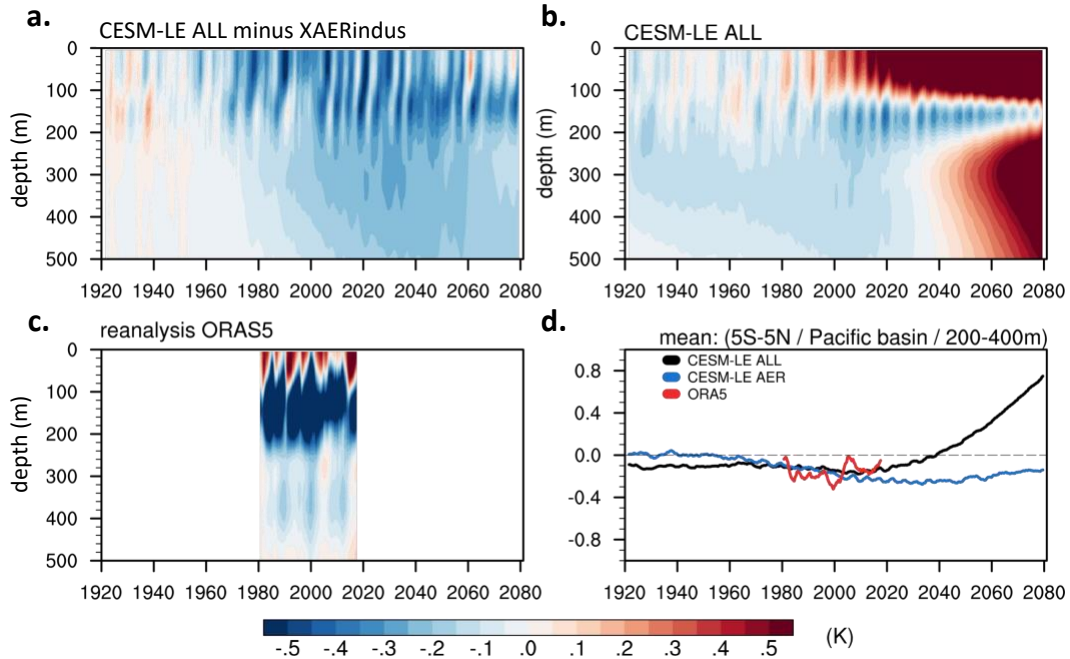


Figure S8. Zonal and meridional mean anomalous potential temperature in the equatorial Pacific (5°S~5°N; Pacific basin) in (a) CESM LE ALL minus XAERindus, (b) CESM LE ALL, and (c) ORAS5 (Ocean Reanalysis System 5 by the European Center for Medium-Range Weather Forecasts²). (d) The averaged anomalous potential temperature in the subsurface equatorial Pacific (5°S~5°N; Pacific basin; 200~400m). The anomalies in CESM LE are computed using the multi-century control simulation with preindustrial condition. The anomalies in ORAS5 are calculated with the base period 1958~1978, a spin-up period treated as a backward extension in ORAS5 system. All of the anomalies are smoothed by a 5-year running mean in CESM AER (All minus XAERindus) and CESM LE, and by 3-year running mean in ORAS5.

SI References

1. H.-Y. Tseng *et al.*, Fast and Slow Responses of the Tropical Pacific to Radiative Forcing in Northern High Latitudes. *Journal of Climate*, 1-31 (2023).
2. Zuo, Hao, et al. "The ECMWF operational ensemble reanalysis–analysis system for ocean and sea ice: a description of the system and assessment." *Ocean science* 15.3, 779-808, (2019).